Scalable fabrication of high-quality crystalline and stable $FAPbI_3$ thin films by combined doctor-blade coat and cation exchange reaction

Sampson Adjokatse, Hong-Hua Fang, Herman Duim, and Maria Antonietta Loi

Zernike Institute for Advanced Materials, University of Groningen, Nijenborgh 4, 9747 AG, Groningen, The Netherlands

Corresponding author: m.a.loi@rug.nl

SUPPORTING INFORMATIOM

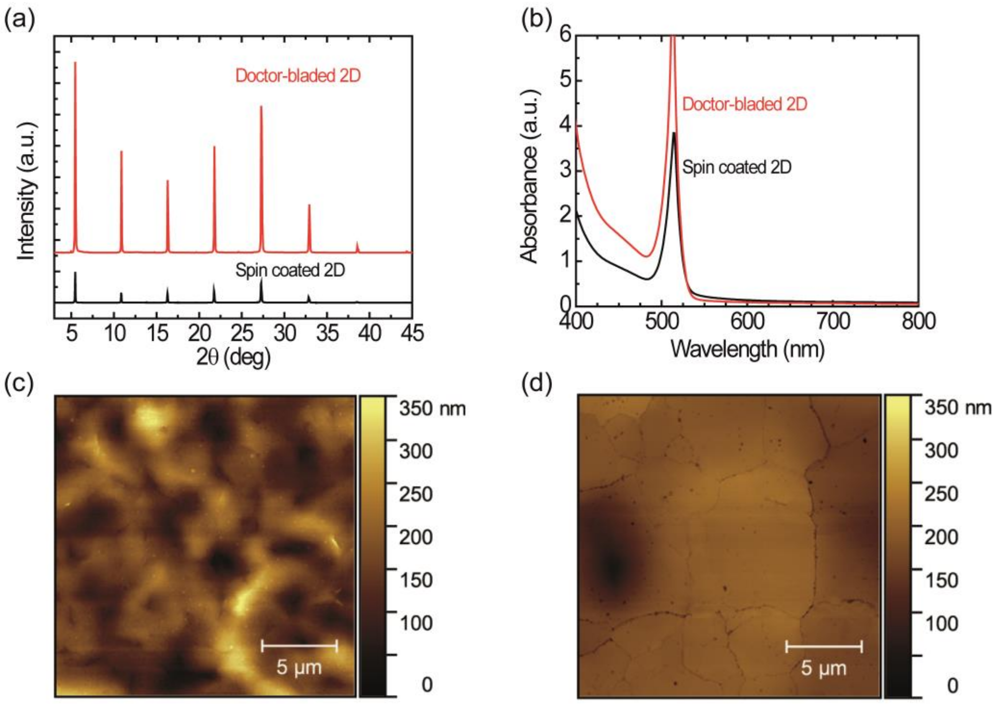

Fig. 1. Structural, optical and morphological characterization of spin coated and doctor-blade coated 2D PEA_2PbI_4 perovskite films on glass substrates. **(a)** X-ray diffraction patterns, **(b)** UV-vis absorbance spectra. AFM topological images of spin coated **(c)** and doctor-blade coated films (**d**).

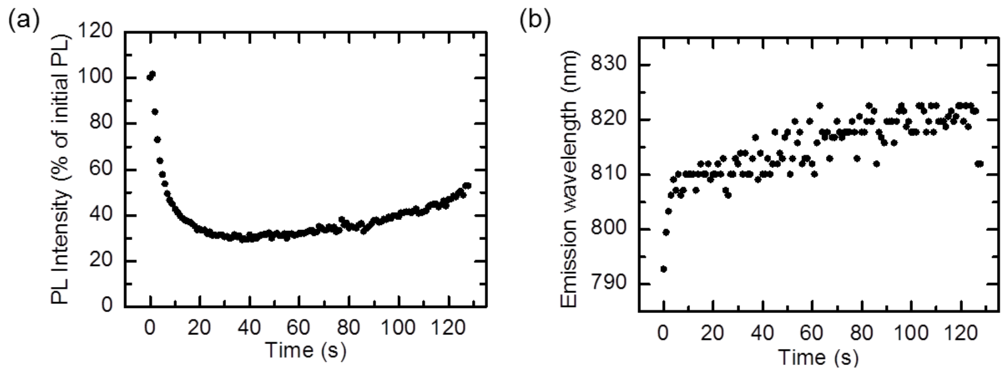

Fig. S2. Results of the Gaussian fitting to the 3D emission peak at different times during the conversion process. (a) The PL intensity normalized to the first occurrence of the 3D emission (100%) and (b) center of gravity of the fitted peak wavelength.

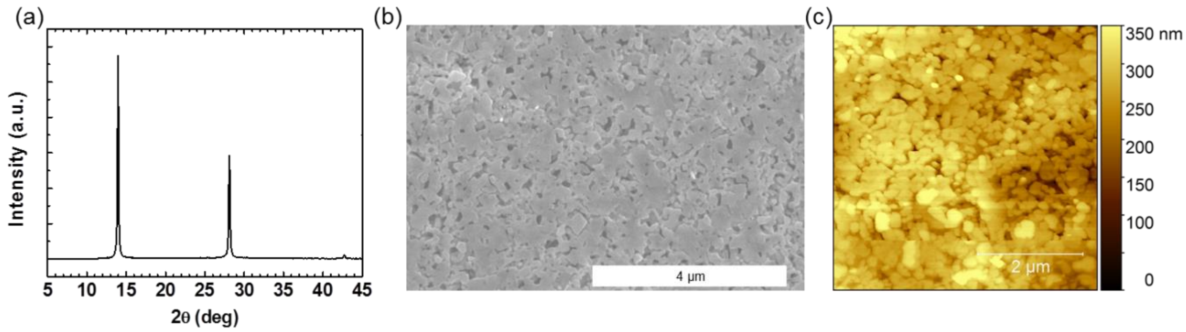

Fig. S3. Structural and morphological characterization of the converted 3D $FAPbI_3$ perovskite film based on spin coated 2D perovskite film. (a) X-ray diffraction pattern, (b) top-view SEM micrograph and (c) AFM image of the film.

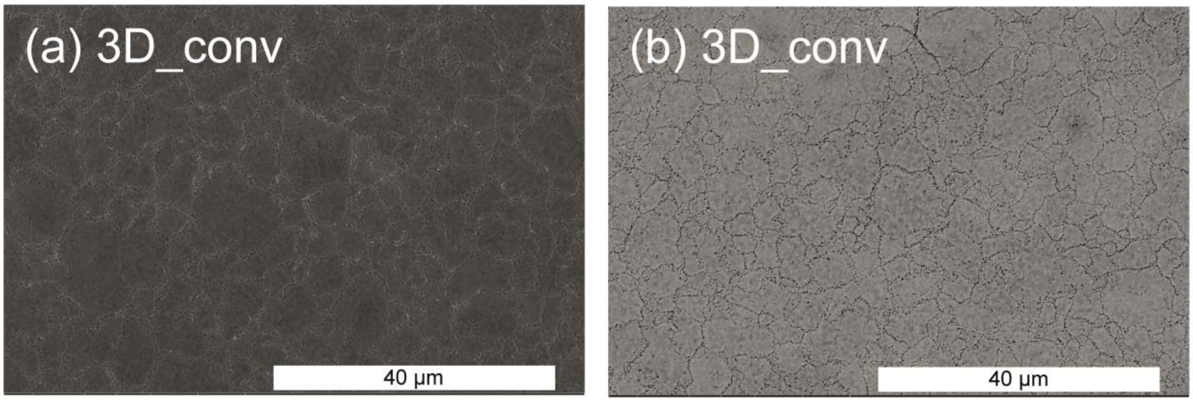

Fig. S4. SEM images showing a wider view of the surface topography and compositional properties of the converted perovskite film.

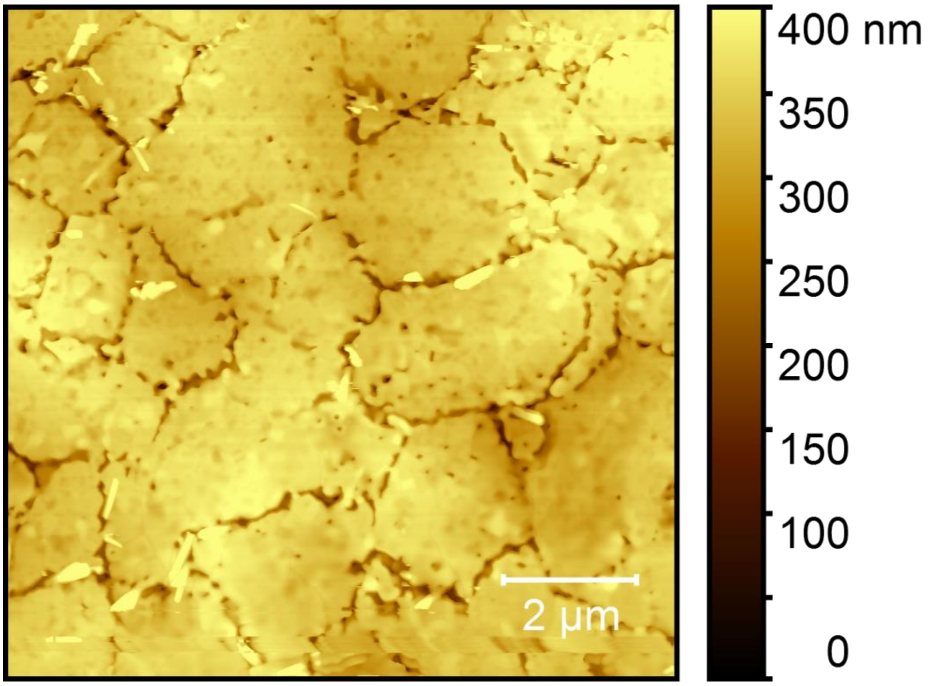

Fig. S5. AFM micrograph of the converted 3D $FAPbI_3$ perovskite film

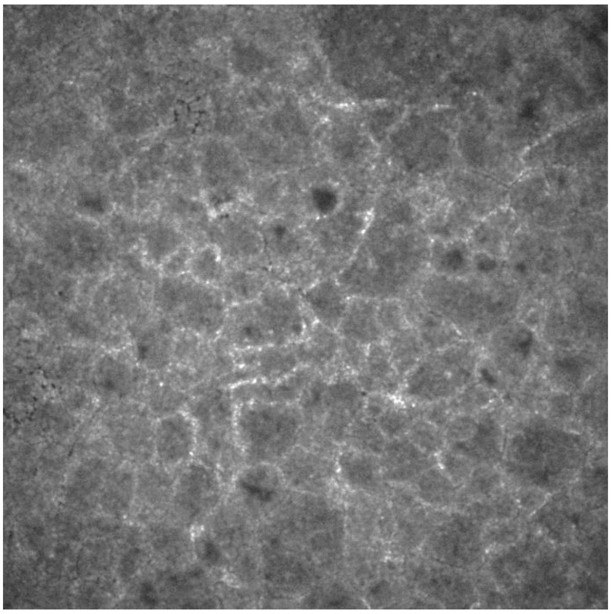

Fig. S6. Confocal laser scanning micrograph of the converted 3D $FAPbI_3$ perovskite film. Brighter colors indicate higher intensity of the PL. The image size is 100 x 100 μm^2.

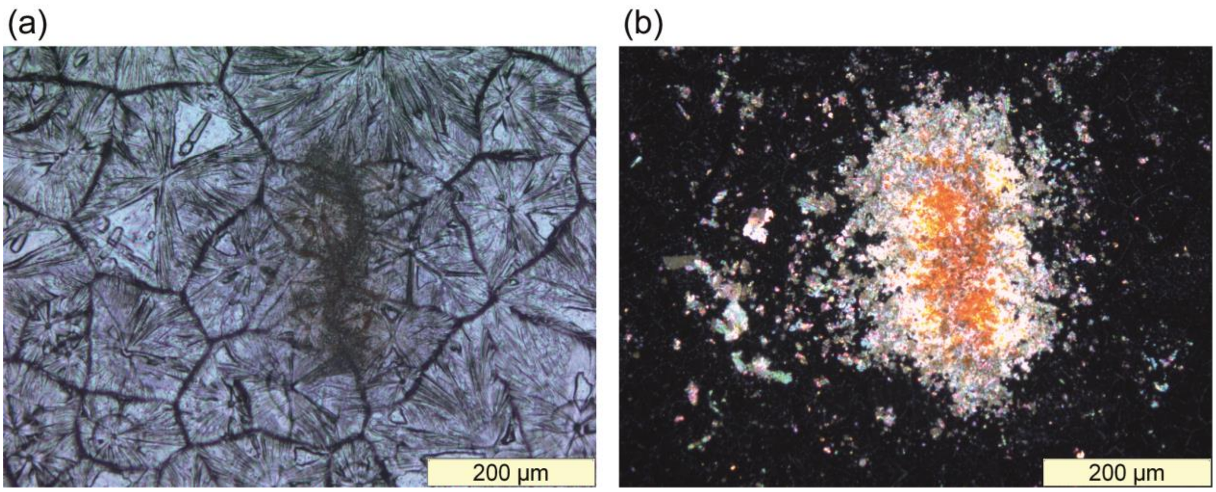

Fig. S7. Bright-field microscopy images showing the decomposition of the reference film under laser excitation (a) without and (b) under cross-polarization.

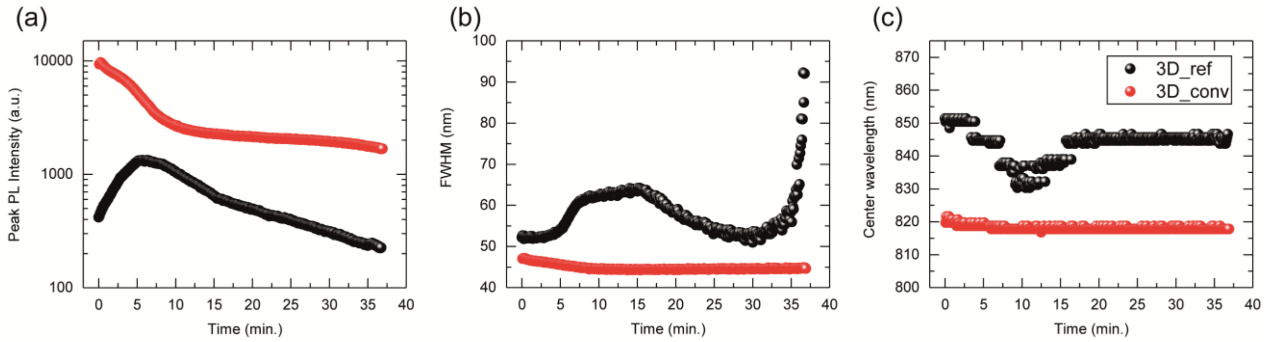

Fig. S8. PL parameters extracted from the data in Fig. 6a and 6b demonstrating the superior film quality of the converted film. **(a)** Peak intensity, **(b)** FWHM, and **(c)** center wavelength of the PL tracked over time. The sharp rise in the FWHM stems from the broad emission feature at high energy.